Thermodynamic and structural behavior of analcime-leucite analogue systems.

Guy L. Hovis, Jacques Roux, Elisabeth Rodrigues

American Mineralogist, Volume 87, pages 523–532, 2002

Thermodynamic and structural behavior of analcime–leucite analogue systems

GUY L. HOVIS,[1,*] JACQUES ROUX,[2] AND ELIZABETH RODRIGUES[3]

[1]Department of Geology and Environmental Geosciences, Lafayette College, Easton, Pennsylvania 18042, U.S.A.
[2]ISTO, CNRS-Université d'Orléans, 1A, rue de la Férollerie, 45071 Orléans cedex 2, France
[3]UFPA–CCEN, Departamento de Química, Rua Augusto Correa no. 1, 66.075-110, Belém, Pará, Brazil

ABSTRACT

Two synthetic solid-solution series, analcime to Rb-leucite and analcime to Cs-leucite (pollucite), have been investigated to understand more fully the thermodynamic and structural behavior of analcime-leucite and similar mineral systems. Unit-cell dimensions and volumes in these series expand with the substitution of analcime component in either Rb-leucite or pollucite, as H_2O molecules structurally replace the smaller entities Rb^{+1} or Cs^{+1}, respectively. Unit-cell volumes vary linearly as functions of composition, but with changing slopes over several segments of compositional space, akin to thermal expansion in K-, Rb-, and Cs-end-member materials studied by previous workers. When symmetry changes displacively from tetragonal to isometric, as in the Rb-bearing series, the slope of volume expansion changes. Once structures have reached full expansion, volume slopes flatten and are little affected by additional analcime component. Enthalpies of solution measured at 50 °C in 20.1 wt% hydrofluoric acid show single-slope linear relationships over the entire compositional ranges of both series. Thus, despite positive volumes of mixing, there are no enthalpies of mixing in either series, nor is there energetic evidence of displacive tetragonal/isometric inversion or the various stages of structural expansion. Overall, the data suggest that the analcime–leucite system also can be modeled as close to thermodynamically ideal. The limited solid solution between natural analcime and leucite must be attributed to energetically favored heterogeneous equilibria involving minerals such as feldspars and other feldspathoids, and not to immiscibility between the end-members.

INTRODUCTION

Thermodynamic mixing properties for solid-solution series provide thermodynamic data for intermediate members of such series and also are critical to an energy-based understanding of mineral behavior. Indeed, positive energies of mixing are generally associated with the phenomenon of exsolution. Mixing properties have been determined in this laboratory for alkali (and Ca-bearing alkali) feldspars having various degrees of Al-Si order, aluminous micas, and nepheline–kalsilite feldspathoids having a range of Si contents (Hovis 1988, 1997; Hovis et al. 1991; Hovis and Roux 1993, 1999; Hovis and Navrotsky 1995; Roux and Hovis 1996; Hovis and Graeme-Barber 1997; Hovis et al. 1999). A potentially valuable addition to data for these series would be mixing properties for the analcime ($NaAlSi_2O_6 \cdot H_2O$)–leucite ($KAlSi_2O_6$) system. Not only would this system provide information on an additional framework silicate series, but it would also give energetic insight into substitutions in mineral series that are necessarily coupled for reasons of structure (discussed below) rather than electrical neutrality.

A difficulty in studying intermediate members of the analcime–leucite system is that naturally occurring specimens display extremely limited solid solution between the end-members (Edgar 1984). Even in experimental studies, analcime shows negligible dissolution of leucite (Edgar 1978). Yet, although leucite containing up to 40 mol% analcime has been produced experimentally at 800 °C (1 atm) by Fudali (1963), leucite containing only 4 mol% analcime is apparently the stable member of high-temperature mineral assemblages in larger chemical systems that include silica content as a variable (Roux and MacKenzie 1978). Moreover, the experimental study of these materials is rendered virtually impossible by phase equilibria that prevent the synthesis of either stable or metastable intermediate compositions.

It is possible to study the analcime–leucite system indirectly by considering analogue substitutions involving Cs and Rb, $Na^{+1}H_2O = \square(Cs^{+1}$ or $Rb^{+1})$. These are systems for which compositionally intermediate members are either known in nature (Černý 1974; Teerstra et al. 1992; Teerstra and Černý 1992) or can be produced in the laboratory. For example, Burley and Roux (unpublished data) found that intermediate members of both Cs- and Rb-bearing systems exhibit conspicuous thermodynamic non-ideality in their unit-cell/molar volumes. These analogue series, therefore, do provide the opportunity to model the thermodynamics of analcime–leucite and to understand the energetics of a structurally coupled substitution between hydrous and anhydrous framework silicate end-members.

CRYSTAL STRUCTURES

The structures of analcime, leucite, and analogue materials such as pollucite ($CsAlSi_2O_6$) have been studied by numerous workers (Taylor 1930; Wyart 1941; Naray-Szabo 1938a, 1938b,

* E-mail: hovisguy@lafayette.edu

0003-004X/02/0004–523$05.00

1942; Callerie and Ferraris 1964; Knowles et al. 1965; Beger 1969; Ferraris et al. 1972; Mazzi et al. 1976; Mazzi and Galli 1978; Palmer et al. 1997). Complete structural summaries can be found in Taylor and Henderson (1968), Hazen and Finger (1979), and Palmer et al. (1997). Palmer (1994) described the general structure of these materials as composed of a network of vertex-sharing $(Al,Si)O_4$ tetrahedra having wide nonintersecting channels parallel to the <111> directions, connected via <110> side-channels. The H_2O molecules of analcime occupy the same structural positions in the <111> channels as the K^{+1} ions in leucite, whereas the Na^{+1} positions of analcime fill sites that are vacant in leucite. (Clearly, H_2O molecules are needed to support the framework structure of analcime, as anhydrous $NaAlSi_2O_6$ exists in nature as the single-chain silicate jadeite.) In a potential solid-solution series from leucite to analcime, the Na cations of analcime would replace vacant sites (□) in leucite as H_2O molecules simultaneously take the positions occupied by K cations in leucite, thus the structural necessity for the coupling $Na^{+1}H_2O = \square K^{+1}$ noted earlier. Written in a structurally analogous style to the formula for analcime ($NaAlSi_2O_6 \cdot H_2O$), then, leucite would be expressed as $\square AlSi_2O_6 \cdot K$.

Despite similarities in structure, the room-temperature symmetries of analcime (isometric or pseudo-isometric; also see additional symmetries discussed by Hazen and Finger 1979) and leucite (tetragonal) are not identical. However, it has long been known that leucite can be converted to isometric symmetry through heating (e.g., Friedel and Friedel 1890; Faust 1963; Taylor and Henderson 1968; Palmer et al. 1997). Taylor and Henderson (1968) describe the structural conversion to isometric symmetry as the untwisting of a collapsed framework. More specifically, Palmer et al. (1997) describe this displacive transformation as the result of the untwisting of tetragonal prisms of corner-linked $(Al,Si)O_4$ tetrahedra about [001]. As these so-called collapsed prisms become untwisted, one can think of the structure as becoming increasingly "expanded."

EXPERIMENTAL PROCEDURES

Sample synthesis and characterization

Two solid-solution series were produced for the present study, one ranging in composition from analcime to pollucite ("Cs-leucite"), the other from analcime to "Rb-leucite" ($RbAlSi_2O_6$). The hydrothermal syntheses were accomplished at CNRS, Orléans, France, by preparing gels of the desired compositions using the method of Hamilton and Henderson (1968), then crystallizing the gels either in an internally heated pressure vessel fitted with a high-performance furnace or in cold-seal vessels. Temperature and pressure conditions (Table 1) ranged from 400 to 800 °C and 2 to 6 kilobars.

Room-temperature powder X-ray diffraction (XRD) analyses of the synthesized materials revealed sharp peaks (similar to those of the NBS Si internal standard) characteristic of well-crystallized materials. Note that K-leucite is tetragonal and isostructural with Rb-leucite, whereas Cs-leucite is isometric or pseudo-isometric at room temperature (see later discussion; also Palmer et al. 1997). Electron microprobe analyses performed at CNRS, Orléans, although somewhat less precise than one would wish due to small grain sizes and alkali ion mobility in these structures, verified the expected chemical compositions of the samples. Water contents of a representative group of samples were checked through weight-loss measurements made on samples of 15 to 40 mg using a Sartorius microbalance (precision of 2 µg, with an estimated standard error of 4 µg, for 50 mg samples). Samples were dried overnight at 100 °C, weighed, slowly dehydrated to 600 °C over a 6 hour period (to prevent sample loss from a fragile gold wrapper), then reweighed. The resulting H_2O contents (Fig. 1) are very close to theoretical values.

Unit-cell dimensions and volumes

Unit-cell dimensions and volumes were determined at CNRS, Orléans, from powder (XRD) data obtained with an Inel CPS120 detector calibrated as outlined in Roux and Volfinger (1996; a few analyses, designated in Table 1, utilized a Siemens diffractometer). The location of each peak was determined by least-squares techniques that resulted in typical uncertainties of 0.007° 2θ. These uncertainties were incorporated into the unit-cell parameter refinements. This procedure, along with inclusion of high-angle data (in excess of 100° 2θ) provided by the INEL system, resulted in low standard errors.

Duplicate studies were carried out on Cs-bearing samples at Lafayette College utilizing a Scintag DMS 2000 automated diffractometer. Scans were made from 12 to 72° 2θ at 0.25°/min utilizing filtered Cu radiation and a monochromator. Cu$K\alpha_2$

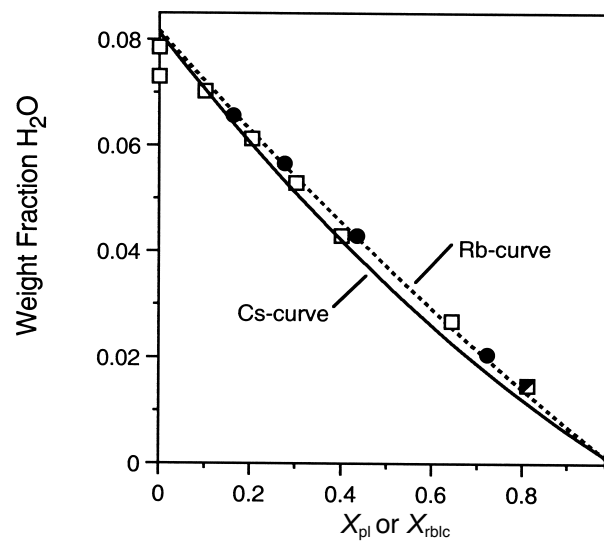

FIGURE 1. Water contents for selected Cs-bearing (squares) and Rb-bearing (circles) samples plotted against mole fraction pollucite or Rb-leucite. The solid (Cs) and dashed (Rb) curves give theoretical weight fractions of water for ideal stoichiometric compositions, whereas symbols give the directly measured water contents. The half-filled square represents a sample for which a minute loss of powder occurred during dehydration and for which the weight-loss experiment would slightly overestimate water content. Note that the pure-analcime samples were used for cell-parameter measurements but not for calorimetry.

TABLE 1. Unit-cell and synthesis data

Sample designation		X_{rblc} or X_{pl} (mole fraction Rb-leucite or pollucite)	a (Å)	V (Å^3)	T (°C)	P (kbar)	Duration (days)
				Analcime end-member			
tniw		0.000	13.7227(3)	2584.13(7)	400	6	6
tra0	*	0.000	13.7192(4)	2582.16(3)	400	2	7
				Rb-bearing series			
rqr0	†	0.087	13.7091(3)	2576.47(6)	600	3.5	5.5
rqqk	†	0.163	13.7003(3)	2571.54(6)	600	3.5	5.5
rqq4	†	0.179	13.6954(4)	2568.75(7)	600	3.5	5.5
rqp0	†	0.276	13.6808(4)	2560.55(7)	600	3.5	5.5
sztk		0.276	13.6820(3)	2561.24(7)	600	3.4	9
szu0		0.379	13.6587(3)	2548.19(5)	600	3.4	9
rqp8	†	0.435	13.6419(4)	2538.75(7)	600	3.5	5.5
szug		0.488	13.6225(5)	2527.97(9)	600	3.4	9
sbz0	†	0.564	13.5914(10)	2510.66(18)	600	3.2	7
sbzg	†‡	0.699	unknown	unknown	600	3.2	7
rqnw	†‡	0.723	unknown	unknown	600	3.5	5.5
rqng	†	0.859	13.3575(23) c = 13.7269(21)	2449.18(43)	600	3.5	5.5
rqn0	†	1.000	13.2930(11) c = 13.7390(21)	2427.76(26)	600	3.5	5.5
				Cs-bearing series			
pqtc	†	0.066	13.7205(1)	2582.92(2)	575	3	2
pqtc	†§	0.066	13.7207(6)	2583.00(31)	575	3	2
pptc	†ll	0.101	13.7191(4)	2582.13(8)	575	3	2
pptc	†§	0.101	13.7200(5)	2582.60(29)	575	3	2
r67g	ll	0.156	13.7166(75)	2581(1.4)	600	2	6.5
pqsg	†	0.204	13.7160(11)	2580.38(21)	475	2.7	15
pqsg	†§	0.204	13.7157(6)	2580.18(34)	475	2.7	15
pqsw	†	0.301	13.7131(4)	2578.75(7)	475	2.7	15
pqsw	†§	0.301	13.7128(7)	2578.54(37)	475	2.7	15
ppts	†§	0.401	13.7128(8)	2578.59(42)	475	2.7	15
ppsw	†§	0.401	13.7147(7)	2579.65(40)	575	3	2
pp28	†ll	0.518	13.7152(20)	2579.94(37)	700	2.7	2
pp28	†§	0.518	13.7123(5)	2578.26(29)	700	2.7	2
r67w	ll	0.553	13.7144(69)	2579(1.3)	600	2	6.5
pp1s	†§	0.645	13.7092(5)	2576.52(28)	700	2.7	2
ijlm		0.667	13.7098(5)	2576.89(9)	700	3	4.5
pp1c	†ll	0.811	13.7002(22)	2571.45(41)	700	2.7	2
pp1c	†§	0.811	13.7015(4)	2572.21(23)	700	2.7	2
tnbs		1.000	13.6803(6)	2560.28(11)	600	5.8	4
pnts	†§	1.000	13.6708(16)	2554.92(91)	800	2	2
9755	†§#	1.000	13.6707(17)	2554.90(96)	800	2	2

Notes: Quantities in parentheses are standard errors in last decimal place(s).
* Synthesis with cold-seal vessel, all others with internally heated pressure vessel.
† Calorimetric sample.
‡ Tetragonal sample, unit-cell parmeters not determinable.
§ Refinement performed at Lafayette College, all others performed at CNRS-Orleans.
ll CNRS-Orleans refinement done with Siemens diffractometer, all others with INEL.
9755 is sample "pnts" after annealing at 1000 °C for 18.4 hours.

peaks were stripped mathematically. Diffraction maxima were determined by Scintag's Peakfinder software. Unit-cell dimensions were calculated utilizing the program of Holland and Redfern (1997) from manually corrected $K\alpha_1$ data based on a Si internal standard (NBS standard reference material 640a having a stated unit-cell dimension of 5.430826 Å). Unit-cell dimensions from the Lafayette study (Table 1) agreed to within two standard errors or better with results from the Inel system, although restriction to lower-angle data resulted in higher standard errors for the Lafayette data.

Solution calorimetry

The calorimetric system used to measure enthalpies of solution has been described by Hovis and Roux (1993) and Hovis et al. (1998). Sample availability did not necessitate the use of sample weights below 46 mg; the average sample weight for all calorimetric experiments was 102 mg. Each sample was dissolved in 910.1 g (about one liter) of 20.1 wt% hydrofluoric acid (HF) at 50 °C under isoperibolic conditions (meaning that the temperature of the medium surrounding the calorimeter was held constant) utilizing an internal sample container (Waldbaum and Robie 1970). Either one or two dissolution experiments were performed in each liter of acid. Multiple experiments in the same solution had no detectable effect on the data, the result of the high dilution of dissolved ions in the acid. Because these samples dissolved rapidly, the calorimetric experiments were conducted on crushed, but not especially fine-grained material (coarser than 200 mesh or 100 µm). This avoided any possibility of heat effects associated with extremely small grain sizes (Nitkiewicz et al. 1983).

UNIT-CELL DATA: RESULTS AND INTERPRETATION

Unit-cell data

Unit-cell dimensions for both Rb and Cs series are given in Table 1. In the case of the Cs-bearing series, all series members were refined as isometric. Standard errors for the pure-Cs calorimetric end-member, however, are greater than those for other compositions. According to Palmer et al. (1997, their Table 8), the displacive phase transformation from tetragonal to isometric symmetry for "Cs-substituted leucite" occurs slightly above room temperature (~100 °C). It may be, therefore, that the Cs end-member of this investigation is actually tetragonal (although pseudo-isometric) and that the higher standard errors result from the averaging of peaks that are slightly split.

The Rb-bearing samples, although isometric for analcime-rich compositions, are tetragonal for members with ≥68.9 mol% Rb. Unit-cell dimensions for samples having 68.9 and 72.3% Rb are not reported because the positions of split peaks are imprecise close to the inversion composition, and also because peak widths are larger than normal even within the context of split peaks. For example, the combined 004/400 diffraction maximum decomposes into two peaks for which half widths at half maximum are more than twice those of the equivalent peaks for tetragonal and isometric samples on either side of these compositions. However, electron microprobe data reveal no chemical inhomogeneity in either sample. Because all phases on this join were synthesized under *P-T* conditions corresponding to isometric symmetry, we conclude that samples at 68.9 and 72.3 mol% Rb have structural complexity related to quenching of the samples, even though one might expect the inversion to be second order. This phenomenon correlates with the observations of Henderson and Taylor (1982), who have described mixed isochemical phases in various feldspathoid solid solutions, including both tetragonal and isometric forms of leucite found to coexist over a 120 °C temperature interval. This finding indicates that these transitions may have a first-order component, even though they are in large part second order.

Interpretation of compositional trends

Unit-cell dimensions and volumes decrease as Na^{+1} and H_2O are replaced by vacancies and Cs^{+1}/Rb^{+1}, respectively (Figs. 2–4). This decrease is consistent with the structural studies noted earlier, which show Na^{+1} ions in analcime occupying vacant sites of the pollucite and Rb-leucite structures. Indeed, if Na^{+1} occupied the Cs^{+1}/Rb^{+1} position in these materials, one might expect unit-cell dimensions and volumes to increase with replacement of Na^{+1} by the relatively larger ions Cs^{+1} and Rb^{+1}. Instead, it is the larger H_2O molecules of analcime that are replaced structurally by the relatively smaller entities Cs^{+1} and Rb^{+1}.

The symmetry change seen in the Rb-bearing series, but not in the Cs-bearing one (except possibly in the pure-Cs end-member), is consistent with the notion that Cs^{+1} ions are large enough to sustain an isometric structure across the entire solid-solution series, structurally compensating for the concomitant decrease in H_2O. A smaller substituent ion such as Rb^{+1}, however, is apparently not large enough to sustain such symmetry. One can predict from the yet smaller size of K^{+1}, therefore, that conversion from isometric to tetragonal symmetry in a theoretical analcime–leucite series would take place at a more analcime-rich composition than observed in the Rb-bearing series.

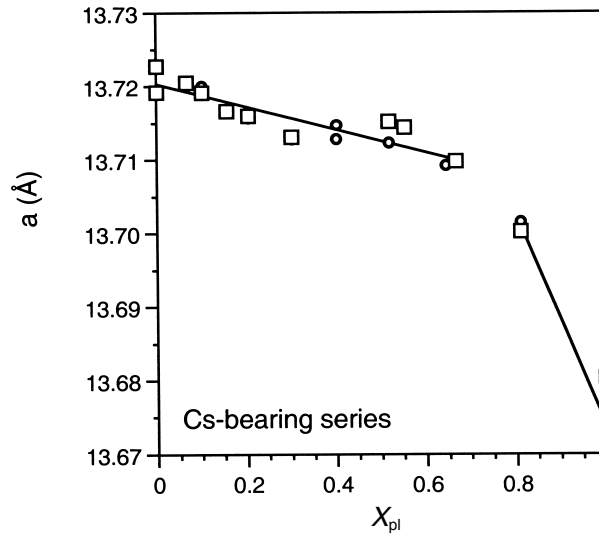

FIGURE 2. The *a* unit-cell dimension of Cs-bearing samples vs. mole fraction pollucite (X_{pl}). Open squares are data measured at CNRS in Orléans, small circles are data measured at Lafayette College. Standard errors are generally smaller than the symbols. Data (Table 1) are divided into linear segments (see text). In comparison with Rb-bearing samples, note that the scale of this diagram is finer than that of Figure 3, as unit-cell dimensions are affected less by Cs than Rb substitution.

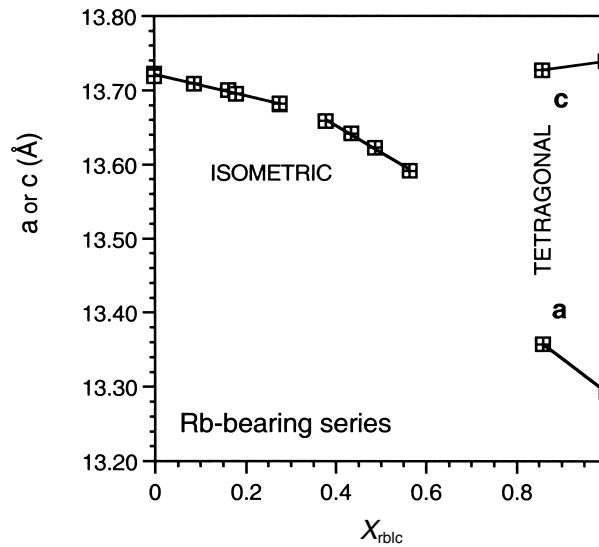

FIGURE 3. The *a* and *c* unit-cell dimensions of Rb-bearing samples vs. mole fraction Rb-leucite (X_{rblc}). All measurements were made at CNRS in Orléans. Standard errors as in Figure 2. Note the change in symmetry from isometric to tetragonal.

Analogy between chemical and thermal expansion

The tetragonal/isometric phase transition associated with compositional change in the analcime–Rb-leucite series mimics the thermal behavior of end-member K-leucite, Rb-leucite,

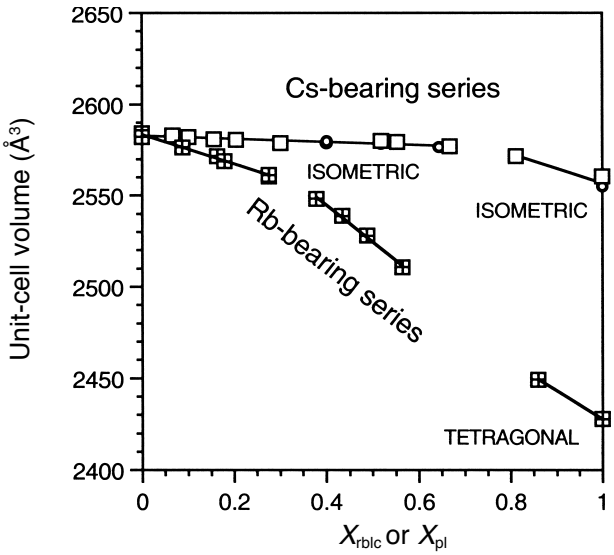

FIGURE 4. Unit-cell volumes vs. mole fraction Rb-leucite or pollucite. Squares with crosses are for members of the Rb series, open squares are Cs-series data, both measured at CNRS, Orléans. Small circles are based on X-ray data collected at Lafayette College for Cs-bearing samples.

and Cs-leucite samples investigated by Taylor and Henderson (1968) and Palmer et al. (1997). The unit-cell data obtained by these authors shows an inversion from tetragonal to isometric symmetry for K-leucite and Rb-leucite as a result of increased temperature. Taylor and Henderson (1968) also identified a second structural change at a temperature above that at which isometric symmetry is achieved. The latter is reflected by flattening of the slope of the *a* dimension (also unit-cell volume) as plotted against temperature, a phenomenon also shown by the high-temperature data of Palmer et al. (1997). Taylor and Henderson (1968) referred to the two temperatures at which slope changes took place as the "inversion" (meaning tetragonal/isometric inversion) temperature (T_i) and the "discontinuity" temperature (T_d), respectively. They attributed the latter to the attainment of a fully expanded tetrahedral framework (also see Hazen and Finger 1979) above which temperature has relatively little effect on expansion, reflected by the flattened slopes of *a* and volume with temperature. This interpretation is supported by Palmer et al. (1997), who ascribe the limited expansion above T_d primarily to the lengthening of T-O bonds (as opposed to the continued untwisting of corner-linked tetrahedra).

Coupled substitutions in the Cs- and Rb-bearing series give series-wide nonlinear variations of *a* and volume as functions of composition (Figs. 2–4), in agreement with earlier observations by Burley and Roux (unpublished). By analogy with the thermal data of Taylor and Henderson (1968) and Palmer et al. (1997), trends for *a* and volume in the analcime–Rb-leucite series can be divided into three linear segments: one tetragonal; a second at mid-composition representing expansion of a partially collapsed structure; and the third at analcime-rich compositions representing a fully expanded structure that is not much affected by the percentage of analcime component.

Taylor and Henderson (1968) modeled $CsAlSi_2O_6$ unit-cell data against temperature using only two linear segments, consistent with the fact that pollucite is isometric (or nearly so) at room temperature. (Note that a third linear segment representing tetragonal symmetry can indeed be seen in the data collected below room temperature by Palmer et al. 1997.) The lower-temperature segment of the data from Taylor and Henderson (1968) represents an isometric structure progressing toward full expansion. With the flattening of the *a* and *V* slopes at T_d the fully expanded structure is little affected by continued temperature increase. Figures 2–4 show a compositional parallel for the analcime–pollucite samples of the present investigation. Both *a* and *V* increase markedly from the pure-Cs end-member toward analcime, then level off at middle compositions once the structure is fully expanded.

It also is instructive to compare changes in the linear trends for cell parameters of the analcime–Rb-leucite and analcime–pollucite series of this investigation with room-temperature data for the three anhydrous (K-Rb-Cs)$AlSi_2O_6$ joins studied by Martin and Lagache (1975; for the K-Cs series, also see Suito et al. 1974). These workers found that a K-Rb leucite series, which is entirely tetragonal at room temperature, displayed one series-wide linear trend in unit-cell volume with composition. In contrast, the Rb-Cs and K-Cs series, both of which switch at middle compositions from tetragonal to isometric symmetry, display linear trends in volume that change slope at the tetragonal/isometric inversion. These points in compositional space, signifying sufficient chemical expansion of the tetragonal structure such that isometric symmetry is achieved, correspond to T_i in the thermal data of Taylor and Henderson (1968). They also correlate with the change in slope and structural inversion observed in the analcime–Rb-leucite series (Fig. 4) of the present study.

Room-temperature symmetry of analcime

Given the comparable effects of temperature and chemistry on the unit-cell parameters of minerals in these systems, as well as the linear variations of these parameters, one can utilize data for K-, Rb-, and Cs-end-member compositions to predict the temperature at which tetragonal analcime is converted to isometric analcime [although it is important to remember that some details of the analcime structure, including the presence of two Na sites (see Palmer 1994), are different from other materials in this group]. Either high-temperature [$V_{i\,(hi\text{-}T)}$] or room-temperature unit-cell volumes [$V_{i\,(rm\text{-}T)}$] at the tetragonal/isometric inversion for K-leucite, Rb-leucite, and Cs-leucite can be plotted against the respective tetragonal/isometric transformation temperatures (T_i) of these materials (data of Palmer et al. 1997). The resulting relationship based on room-temperature data (Fig. 5) is expressed as

$$T_i\ (°C) = 6983\ (440) - 2.69\ (0.18)\ V_{i\,(rm\text{-}T)}\ (Å^3) \quad (1)$$

(where bracketed quantities for this and subsequent equations are standard errors of the coefficients). If one substitutes the room-temperature unit-cell volume of analcime (2584 Å^3, Table 1) into Equation 1, a T_i of 38 °C (shown on Fig. 5) is obtained. (The same calculation utilizing the high-temperature line and

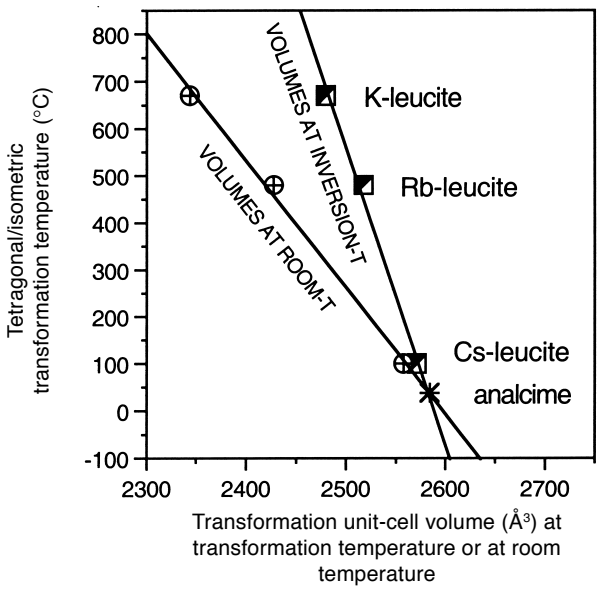

FIGURE 5. High-temperature (squares) and room-temperature (circles) tetragonal/isometric transformation volumes plotted against transformation temperature for K-leucite, Rb-leucite, and Cs-leucite from the data of Palmer et al. (1997). The line for room-temperature data corresponds to Equation 1.

the room-temperature volume for analcime gives a nearly coincidental T_i of 30 °C. Strictly speaking, the use of room-temperature data in conjunction with the high-temperature line is improper, but the resulting T_i of 30 °C indicates that the "high-temperature" inversion volume is nearly equal to room temperature, in agreement with the previous calculation.) Thus, a specimen of analcime whose site occupancies allow for isometric symmetry (see Mazzi and Galli 1978; Hazen and Finger 1979) is likely to be near tetragonal/isometric inversion at room temperature. Even the slightest solid solution for such a sample could change T_i a few degrees in either direction. It is not surprising, then, that some room-temperature samples of natural analcime actually are isometric, whereas others are pseudo-isometric and tetragonal (Mazzi and Galli 1978; Hazen and Finger 1979). Indeed, symmetry may vary according to whether one is observing the relevant outcrop in summer or winter!

Volumes of mixing

A primary goal of this work was to model the thermodynamic mixing properties for these analogue series. Although volumes can be expressed for both series utilizing a succession of linear segments, excess volumes are mathematically more usable when configured as a continuous curve. Such curves for unit-cell volume are shown in Figure 6, with corresponding equations for Cs- and Rb-bearing series of

$$V\ (\text{Å}^3/\text{unit cell}) = 2584.13\ (0.01) - 35\ (4)\ X_{pl} + 92\ (13)\ X_{pl}^2 - 84\ (9)\ X_{pl}^3 \quad (2)$$

$$V\ (\text{Å}^3/\text{unit cell}) = 2584.13\ (0.01) - 30\ (13)\ X_{rblc} - 230\ (44)\ X_{rblc}^2 + 101\ (33)\ X_{rblc}^3 \quad (3)$$

where X expresses mole fractions of the end-members, "pl" for pollucite and "rblc" for Rb-leucite. Note that both series have been forced to converge to the same point at the Na ends of the series by giving a high weight to the pure-analcime data.

The corresponding volumes of mixing (V_{ex}; Fig. 7) express differences between the observed volumes and chemically equivalent "ideal" mechanical mixtures of the end-members. These are given below as third-order polynomials using Margules notation:

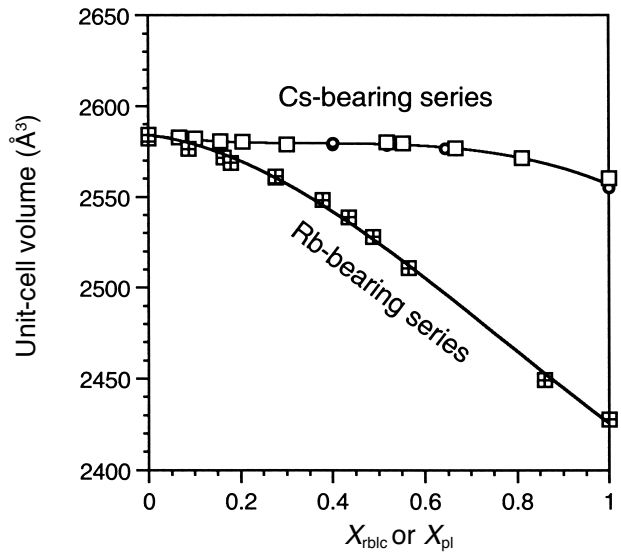

FIGURE 6. Unit-cell volumes analyzed as continuous functions of mole fraction Rb-leucite or pollucite, with symbols as in Figure 4. The plotted curves correspond to Equations 2 and 3.

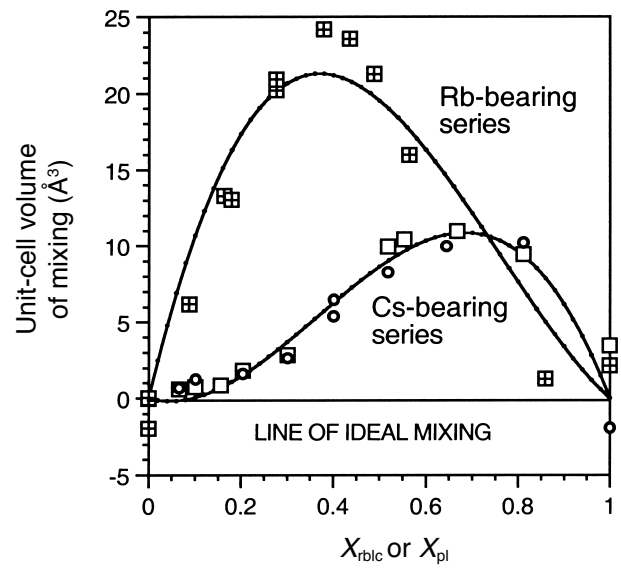

FIGURE 7. Unit-cell volumes of mixing derived from the curves of Figure 6 and corresponding to Equations 4 and 5. Symbols as in Figure 4.

$$V_{ex}\ (\text{Å}^3/\text{unit cell}) = -7.9\ (4.2)\ X_{pl}\ X^2_{anal} + 77\ (5)\ X_{anal}\ X^2_{pl} \quad (4)$$

$$V_{ex}\ (\text{Å}^3/\text{unit cell}) = 129\ (11)\ X_{rblc}\ X^2_{anal} + 27\ (16)\ X_{anal}\ X^2_{rblc} \quad (5)$$

where X_{anal} is mole fraction analcime. The reversed asymmetries for V_{ex} in the two series are easily explained as functions of the different expansion rates. Again, these are related to the presence of a tetragonal/isometric inversion in the Rb-bearing series that is not present in the Cs-bearing series (except possibly for pollucite itself), and also to the attainment of full expansion of the tetrahedral framework at a more analcime-rich composition in the Rb than in the Cs series.

CALORIMETRIC DATA: RESULTS AND INTERPRETATION

Calorimetric data

Enthalpies of solution for the Cs and Rb series are reported in Table 2 and Figure 8. In order to gain a sense for calorimetric precision, twice the standard deviation of the heats of solution for all experiments on each sample was computed, then divided by the average heat of solution for the sample. The resulting values for precision range for various samples from 0.03 to 0.45% of the heat-of-solution values. Average reproducibility among all samples is 0.16%, which is among the higher degrees of precision ever observed in this laboratory.

TABLE 2. Calorimetric data

Sample designation	Run number		X_{rblc} or X_{pl} (mole fraction Rb-leucite or pollucite)	Gram formula weight of sample (g)	Sample weight (g)	Temperature increase during dissolution (°C)	C_P before* (J/°C)	C_P after† (J/°C)	Enthalpy before‡ (kJ/mol)	Enthalpy after§ (kJ/mol)
Rb-bearing series										
rqro	834		0.087	224.0323	0.09869	0.056602	3873.8	3874.6	–496.74	–496.85
rqro	858		0.087	224.0323	0.07017	0.040321	3872.2	3871.5	–497.49	–497.39
rqqk	842	#	0.163	227.4117	0.06091	0.034250	3870.6	3871.2	–493.97	–494.04
rqqk	855	#	0.163	227.4117	0.06005	0.033743	3871.7	3872.3	–493.77	–493.84
rqq4	838	#	0.179	228.1187	0.07955	0.044778	3869.7	3870.8	–495.90	–496.04
rqq4	860		0.179	228.1187	0.07237	0.040068	3875.1	3875.2	–493.32	–493.32
rqq4	866		0.179	228.1187	0.05134	0.028793	3875.3	3875.3	–494.80	–494.81
rqpo	837		0.276	232.4362	0.09105	0.050086	3873.1	3874.6	–494.23	–494.43
rqpo	859		0.276	232.4362	0.07140	0.039236	3873.6	3873.2	–493.79	–493.74
rqp8	840	#	0.435	239.4883	0.07386	0.039324	3869.7	3870.6	–492.43	–492.54
rqp8	864		0.435	239.4883	0.07015	0.037245	3874.8	3874.0	–491.70	–491.60
sbzo	836		0.564	245.2421	0.05160	0.026660	3873.7	3873.8	–489.85	–489.86
sbzo	863	#	0.564	245.2421	0.05153	0.026592	3870.7	3870.7	–488.88	–488.89
sbzg	835	#	0.699	251.2226	0.08547	0.042975	3870.9	3871.7	–487.99	–488.09
sbzg	861	#	0.699	251.2226	0.06151	0.030948	3870.6	3870.9	–488.26	–488.29
rqnw	841		0.723	252.2898	0.08542	0.042773	3874.3	3874.5	–488.46	–488.48
rqnw	856		0.723	252.2898	0.07947	0.039774	3875.7	3875.2	–488.40	–488.33
rqng	839		0.859	258.3637	0.08193	0.039835	3873.5	3874.4	–485.61	–485.73
rqng	862		0.859	258.3637	0.07477	0.036168	3875.3	3874.6	–483.35	–483.27
rqng	867	#	0.859	258.3637	0.04592	0.022311	3873.0	3872.9	–485.21	–485.20
rqno	857	#	1.000	264.6199	0.07254	0.034304	3871.5	3871.8	–483.50	–483.55
rqno	865	#	1.000	264.6199	0.05019	0.023757	3870.4	3870.6	–483.81	–483.84
Cs-bearing series										
pqtc	779		0.066	226.2213	0.14920	0.084210	3872.9	3873.3	–493.52	–493.56
pqtc	784	#	0.066	226.2213	0.10127	0.057213	3868.6	3872.0	–493.44	–493.86
pptc	766		0.101	229.4645	0.15642	0.086886	3871.9	3872.4	–492.54	–492.58
pptc	789		0.101	229.4645	0.10640	0.059120	3875.4	3874.4	–493.13	–493.00
pqsg	780	#	0.204	238.9210	0.15323	0.081440	3871.0	3871.9	–490.58	–490.67
pqsg	786		0.204	238.9210	0.10645	0.056519	3873.7	3873.6	–490.42	–490.39
pqsw	781		0.301	247.8169	0.15192	0.076931	3874.2	3875.9	–485.23	–485.42
pqsw	783		0.301	247.8169	0.12124	0.061386	3873.5	3874.2	–485.06	–485.12
ppts	768		0.401	256.9885	0.16507	0.080691	3873.0	3872.6	–485.58	–485.50
ppts	788		0.401	256.9885	0.10545	0.051566	3874.1	3872.3	–485.90	–485.65
ppsw	765		0.401	257.0252	0.15450	0.075816	3868.7	3869.2	–486.99	–487.03
ppsw	791		0.401	257.0252	0.10445	0.051092	3874.7	3874.5	–486.19	–486.13
pp28	763	#	0.518	267.7775	0.15919	0.074454	3868.9	3868.5	–483.58	–483.51
pp28	790	#	0.518	267.7775	0.10574	0.049345	3870.9	3872.7	–482.75	–482.92
1p1s	761	#	0.645	279.3845	0.15133	0.067498	3868.2	3868.9	–481.08	–481.15
1p1s	778	#	0.645	279.3845	0.15255	0.067973	3868.9	3869.5	–480.68	–480.74
pp1c	759	#	0.811	294.6674	0.14036	0.058673	3869.8	3870.4	–475.73	–475.78
pp1c	782	#	0.811	294.6674	0.13473	0.056323	3871.9	3871.5	–476.01	–475.95
pnts	755		1	312.0549	0.15026	0.058697	3874.0	3874.0	–471.32	–471.28
pnts	785		1	312.0549	0.10857	0.042526	3872.2	3874.2	–472.35	–472.58
pnts	792		1	312.0549	0.12303	0.048271	3873.6	3873.4	–473.33	–473.29
9755	767	#	1	312.0549	0.15279	0.060044	3868.8	3869.2	–473.49	–473.49
9755	787		1	312.0549	0.10768	0.042253	3873.7	3873.9	–473.38	–473.40

* Calorimeter heat capacity before dissolution.
† Calorimeter heat capacity after dissolution.
‡ Enthalpy of solution based on heat capacity before dissolution.
§ Enthalpy of solution based on heat capacity after dissolution.
# Calorimetric experiment using same acid as in the preceding experiment.

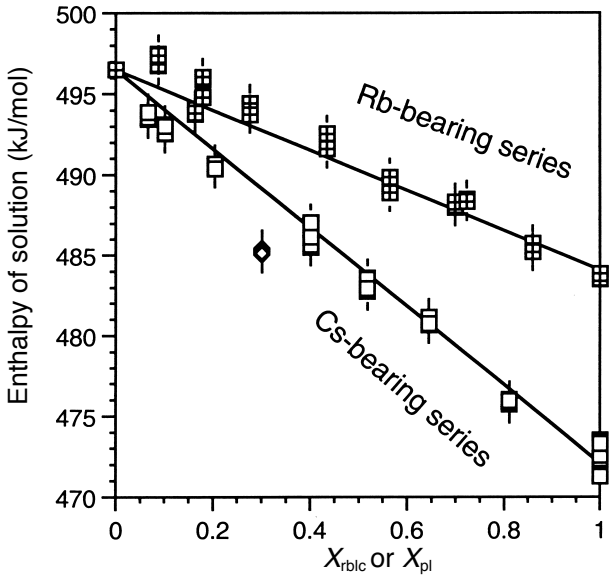

FIGURE 8. Enthalpies of solution for Rb- and Cs-bearing series vs. mole fraction Rb-leucite or pollucite. All dissolutions were carried out at 50.0 °C. Symbols as in Figure 4, except that diamonds are for a Cs-series sample whose data fall off the fitted line. The lines correspond to Equations 6 and 7.

Trends in calorimetric data and the absence of excess enthalpies

Data for the Cs-bearing series are fit well by a linear relationship between enthalpy of solution ($-H_{soln}$) and composition:

$$-H_{soln}\ (\text{kJ/mol}) = 496.50\ (0.01) - 24.4\ (0.2)\ X_{pl}. \quad (6)$$

Note that data for the sample at $X_{pl} = 0.301$ do not fall along this line and were not used in the calculation. Although there is no basis from X-ray or unit-cell data to doubt the quality of the latter sample, past experience suggests that the sample might have contained an impurity, perhaps unreacted synthesis materials. There can be little doubt, however, that the data define a linear trend. This correlates with the absence of enthalpies of mixing at all compositions. Indeed, enthalpies of mixing of low magnitude are consistent with the very small Gibbs energies of mixing (Fig. 9) calculated from the aqueous ion-exchange data of Lagache (1995) for similar crystalline solutions.

The Rb-bearing series exhibits similar behavior. Calorimetric data are fit well by a linear relationship between heats of solution and composition:

$$-H_{soln}\ (\text{kJ/mol}) = 496.50\ (0.01) - 12.5\ (0.3)\ X_{rblc}. \quad (7)$$

Even though this series undergoes a symmetry change at a composition between 56.4 and 68.9 mol% Rb, there is no hint from the tightly constrained calorimetric data of an energy effect related to tetragonal/isometric inversion, nor do the two tetragonal samples closest to the inversion composition (noted earlier as having finely split X-ray peaks) give calorimetric evidence of structural complexity.

Note that no calorimetric data could be collected for pure analcime. This was a result of the experimental difficulty of synthesizing an impurity-free sample for the calorimetric investigation, even though two analcime samples were indeed produced for unit-cell work. Without such data, independent least-squares analyses of the Rb- and Cs-calorimetric data were unlikely to produce lines that intersected the pure-analcime ends of the two series at a common point. Equations 6 and 7, therefore, were constrained to produce such agreement. Even so, the analyses produced values for r^2 of 0.996 and 0.983, respectively, for the two equations. It is clear, then, that enthalpies of mixing for both series are either zero or hidden within the very small standard deviations of the calorimetric data.

DISCUSSION

Close parallels can be drawn between the behavior of unit-cell dimensions/volumes for the analcime–pollucite and analcime–Rb-leucite solid solution series of the present work, the thermal behavior of end-members leucite/Rb-leucite/pollucite (Taylor and Henderson 1968; Palmer et al. 1997), and room-temperature chemical effects in K-Rb/K-Cs/Rb-Cs leucite binary series (Martin and Lagache 1975). Transformation from tetragonal to isometric symmetry in all cases is apparently achieved as a function of tetrahedral framework expansion (according to Palmer et al. 1997, via the untwisting of tetragonal prisms of corner-linked $(Al,Si)O_4$ tetrahedra about [001]) through either chemical or thermal means. Once isometric symmetry has been achieved, further framework expansion occurs at a subdued rate, reflected by the flattening of unit-cell dimension/volume trends on plots against temperature or com-

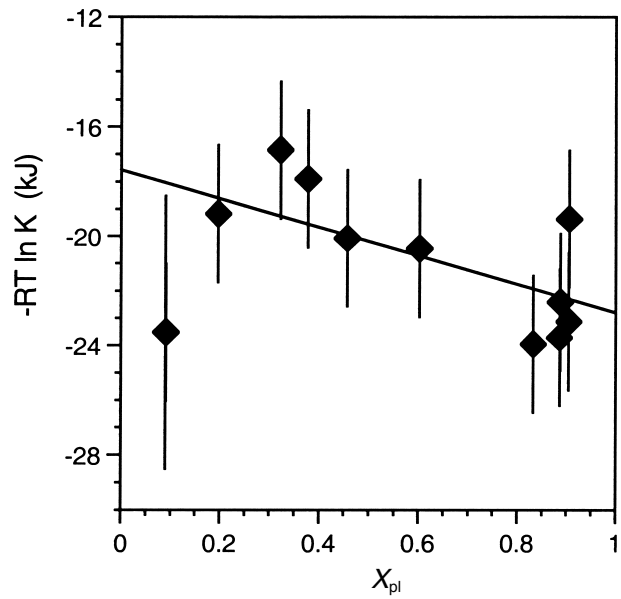

FIGURE 9. Calculation of thermodynamic parameters from the aqueous ion-exchange data of Lagache (1995). The slope of the fitted line implies a Margules parameter for the Gibbs free energy of mixing of 2.6 kJ/mol, based on a regular-solution model. This translates into an excess Gibbs free energy of only 650 J/mol at $X_{pl} = 0.5$.

position. For the two analogue series reported in the present study, expansion is associated with the addition of H_2O molecules in place of Cs^{+1} or Rb^{+1}, concomitant with an increase in analcime component.

Positive volumes of mixing clearly exist for both of the analogue series. Magnitudes of V_{ex} increase from the Cs-bearing to the Rb-bearing series. It seems reasonable to attribute this to the increased size contrast between substituting species, H_2O-Cs^{+1} vs. H_2O-Rb^{+1}. One could predict that the volumes of mixing for an analcime–K-leucite system would be even greater in magnitude than for the Rb-series, and maximized toward even more analcime-rich compositions, as size contrast would increase for H_2O-K^{+1} substitution.

Despite the structural changes evidenced by the unit-cell data for analcime–Rb-leucite and analcime–pollucite, the enthalpies of solution show linear trends having a single slope across each series. For the Rb-bearing series, there is no noticeable energy effect associated with the change from tetragonal to isometric symmetry, entirely in keeping with the displacive nature of the transformation. Moreover, based on failure of the calorimetric data for the Rb-series to change slope at the transformation composition (Fig. 7), one of two scenarios seems likely. Perhaps the energies associated with pre-transition framework expansion related to the untwisting of tetrahedral components of the structure are similar in magnitude to those associated with post-transition expansion that is the result of T-O bond lengthening (Palmer et al. 1997). Or, maybe the various expansion processes are coupled at a linearly changing rate as the style of structural expansion changes across the solid solution series.

Whatever the explanation for the linear trends of the calorimetric data, enthalpies of mixing in these systems are not detectable at the conditions of the calorimetric measurements (50 °C), despite the high precision of the data. Unlike systems such as alkali feldspars (Hovis 1988) or muscovite–paragonite micas (Roux and Hovis 1996), there is no enthalpic evidence of strain energy associated with intermediate compositions of the series. Barring excess heat capacities above 50 °C for these materials, the only mechanism through which significant Gibbs free energies of mixing could be generated is through PV_{ex} energy. In such a case, immiscibility in these systems could only be associated with high pressure.

Based on the analogue systems studied here, one can reasonably model the enthalpic behavior of the analcime–leucite system as ideal, or nearly so. Thus, geologic environments within the earth's crust should reflect complete miscibility between the end-members. The absence of mid-compositional members of this mineral series in nature, therefore, cannot be ascribed to strain related to analcime substitution in leucite, or vica versa. Rather, their absence must be related to heterogeneous phase equilibria beyond the analcime–leucite system, in all likelihood ones involving feldspars and other feldspathoids, which energetically favor the formation of alternative mineral assemblages.

Finally, data for the analcime–Rb-leucite and analcime–pollucite systems form an interesting contrast with the mixing properties of other mineral series studied in this laboratory. Alkali feldspars (Hovis 1988, 1997; Hovis and Navrotsky 1995; Hovis and Graeme-Barber 1997; Hovis et al. 1999) and muscovite–paragonite micas (Roux and Hovis 1996) exhibit positive volumes of mixing that are accompanied by positive enthalpies of mixing. Middle compositions of the nepheline–kalsilite system (Hovis and Roux 1993, 1999) show positive enthalpies of mixing, but no volumes of mixing. Now analcime–leucite analogue systems display positive volumes of mixing, yet no enthalpies of mixing. Collectively these behaviors are a reminder that positive volumes and enthalpies of mixing do not always go hand-in-hand. Apparent "physical nonideality" is not necessarily accompanied by "thermal nonideality." In the case of analcime–leucite analogue systems, structural expansion produces multiple linear segments in the volume properties that give positive volumes of mixing relative to end-member compositions. Either because of energetic coupling or the similarity in energy magnitudes of various expansion processes, however, expansion is not accompanied by excess enthalpies resulting from structural strain, nor apparently by immiscibility for intermediate members of these series.

ACKNOWLEDGMENTS

It seems especially appropriate to contribute this paper to a volume that honors Mike Holdaway, who has had a deep and long-held interest in the connections among mineral chemistry, thermodynamics, and phase equilibria. We are pleased to be a part of this tribute. G.H. gratefully acknowledges support for this research by the National Science Foundation through grants EAR-9613710 and EAR-0000523 and by Lafayette College through funds for the John H. Markle professorship. E.R. acknowledges support of her Ph.D. thesis by CNPq through grant 2002 14-97/7. We thank associate editor Barbara Dutrow and reviewers C.M.B. Henderson and Bill Carey for their excellent and helpful reviews of this manuscript.

REFERENCES CITED

Beger, R.M. (1969) The crystal structure and chemical composition of pollucite. Zeitschrift für Kristallographie, 129, 280–302.

Callerie, M. and Ferraris, G. (1964) Structtura dell'analcime $NaAlSi_2O_6·H_2O$. Atti Accademia delle Scienze di Torino, 98, 821–846.

Černý, P. (1974) The present status of the analcime-pollucite series. Canadian Mineralogist, 12, 334–341.

Edgar, A.D. (1978) Subsolidus phase relations in the system $NaAlSi_2O_6$-$KAlSi_2O_6$ at 1 kb P_{H_2O} and their bearing on the origin of pseudoleucites and analcime in igneous rocks. Neues Jahrbuch für Mineralogie Monatshefte, H5, 210–222.

———(1984) Chemistry, occurrence, and paragenesis of feldspathoids: A review. In W.L. Brown, Ed., Feldspars and Feldspathoids, p. 501–532. Reidel, Dordrect.

Faust, G.T. (1963) Phase transition in synthetic and natural leucite. Schweizerische Mineralogische und Petrographische Mitteilungen, 43, 165–195.

Ferraris, G., Jones, D.W., and Yerkess, Y. (1972) A neutron-diffraction study of the crystal structure of analcime, $NaAlSi_2O_6·H_2O$. Zeitschrift für Kristallographie, 135, 240–252.

Friedel, C. and Friedel, G. (1890) Action des alcalis and des silicates alcalins sur le mica, production de nepheline, de l'amphigene, de l'orthose. Bulletin de la Société Française de Minéralogie, 13, 129–139.

Fudali, R.F. (1963) Experimental studies bearing on the origin of pseudoleucite and associated problems of alkalic rock genesis. Geological Society of America Bulletin, 74, 1101–1126.

Hamilton, D.L. and Henderson, C.M.B. (1968) The preparation of silicate composition by a gelling method. Mineralogical Magazine, 36, 832–838.

Hazen, R.M. and Finger, L.W. (1979) Polyhedral tilting: A common type of pure displacive phase transition and its relationship to analcite at high pressure. Phase Transitions, 1, 1–22.

Henderson, C.M.B. and Taylor, D. (1982) The structural behavior of the nepheline family: (1) Sr and Ba aluminates (MAl_2O_4). Mineralogical Magazine, 45, 111–127.

Holland, T.J.B. and Redfern, S.A.T. (1997) Unit-cell refinement: Changing the dependent variable, and use of regression diagnostics. Mineralogical Magazine, 61, 65–77.

Hovis, G.L. (1988) Enthalpies and volumes related to K-Na mixing and Al-Si order/disorder in alkali feldspars. Journal of Petrology, 29, 731–763.

———(1997) Hydrofluoric acid solution calorimetric investigation of the effect of anorthite component on enthalpies of K-Na mixing in feldspars. American Mineralogist, 82, 149–157.

Hovis, G.L. and Graeme-Barber, A. (1997) Volumes of K-Na mixing for low albite-microcline crystalline solutions at elevated temperature: A test of regular solution thermodynamic models. American Mineralogist, 82, 158–164.

Hovis, G.L. and Navrotsky, A. (1995) Enthalpies of mixing for disordered alkali feldspars at high temperature: A test of regular solution thermodynamic models and a comparison of hydrofluoric acid and lead borate solution calorimetric techniques. American Mineralogist, 80, 280–284.

Hovis, G.L. and Roux, J. (1993) Thermodynamic mixing properties of nepheline-kalsilite crystalline solutions. American Journal of Science, 293, 1108–1127.

———(1999) Thermodynamics of excess silicon in nepheline and kalsilite crystalline solutions. European Journal of Mineralogy, 11, 815–827.

Hovis, G.L., Delbove, F., and Roll Bose, M. (1991) Gibbs energies and entropies of K-Na mixing for alkali feldspars from phase equilibrium data: Implications for feldspar solvi and short-range order. American Mineralogist, 76, 913–927.

Hovis, G.L., Roux, J., and Richet, P. (1998) A new era in hydrofluoric acid solution calorimetry: Reduction of required sample size below ten milligrams. American Mineralogist, 83, 931–934.

Hovis, G.L., Brennan, S., Keohane, M., and Crelling, J. (1999) High-temperature X-ray investigation of sanidine-analbite crystalline solutions: Thermal expansion, phase transitions, and volumes of mixing. Canadian Mineralogist, 37, 701–709.

Knowles, C.R., Rinaldi, F.F., and Smith, J.V. (1965) Refinement of the crystal structure of analcime. Indian Mineralogist, 6, 127–140.

Lagache, M. (1995) New experimental data on the stability of the pollucite-analcime series: application to natural assemblages. European Journal of Mineralogy, 7, 319–323.

Martin, R.F. and Lagache, M. (1975) Cell edges and infrared spectra of synthetic leucites and pollucites in the system $KAlSi_2O_6$-$RbAlSi_2O_6$-$CsAlSi_2O_6$. Canadian Mineralogist, 13, 275–281.

Mazzi, F. and Galli, E. (1978) Is each analcime different? American Mineralogist, 63, 448–460.

Mazzi, F., Galli, E., and Gottardi, E. (1976) The crystal structure of tetragonal leucite. American Mineralogist, 61, 108–115.

Naray-Szabo, St.V. (1938a) Die struktur des pollucits $CsAlSi_2O_6{\cdot}H_2O$. Zeitschrift für Kristallographie, 99, 277–282.

———(1938b) Note on the structure of analcite. Zeitschrift für Kristallographie, 99, 291.

———(1942) Die struktur des pollucits $CsAlSi_2O_6$. Zeitschrift für Kristallographie, 104, 39–44

Nitkiewicz, A.M., Kerrick, D., and Hemingway, B.S. (1983) The effect of particle size on enthalpy of solution of quartz. Geological Society of America Annual Meeting, Abstracts with Programs, 15, 653.

Palmer, D.C. (1994) Crystal Maker: Interactive crystallography for Macintosh and Power Macintosh. Lynxvale Ltd., Cambridge, U.K.

Palmer, D.C., Dove, M.T., Ibberson, R.M., and Powell, B.M. (1997) Structural behavior, crystal chemistry, and phase transitions in substituted leucite: High-resolution neutron powder diffraction studies. American Mineralogist, 82, 16–29.

Roux, J. and Hovis, G.L. (1996) Thermodynamic mixing models for muscovite-paragonite solutions based on solution calorimetric and phase equilibrium data. Journal of Petrology, 37, 1241–1254.

Roux, J. and MacKenzie, W.S. (1978) Sodium in leucite and its petrogenetic significance: An experimental study. Bulletin de la Société Française de Minéralogie et Cristallographie, 10, 478–484.

Roux, J. and Volfinger, M. (1996) Mesures précises à l'aide d'un détecteur courbe. Journal de Physique IV, colloque C4, 6, 36–42.

Suito, K., Lacam, A., and Iiyama, J.T. (1974) Stabilité des solutions solides de la série pollucite-leucite sous une pression d'eau de 30 kb. Comptes Rendus de l'Académie des Sciences Paris, 278, série D, 2397–2400.

Taylor, D. and Henderson, C.M.B. (1968) The thermal expansion of the leucite group of minerals. American Mineralogist, 53, 1476–1489.

Taylor, W.H. (1930) The structure of analcite ($NaAlSi_2O_6{\cdot}H_2O$). Zeitschrift für Kristallographie, 74, 1–19.

Teerstra, D.K. and Černý, P. (1992) Controls on the morphology of analcime-pollucite in natural minerals, synthetic phases, and nuclear waste products. Crystral Research and Technology, 27, 931–939.

Teerstra, D.K., Černý, P., and Chapman, R. (1992) Compositional heterogeneity of pollucite from High Grade Dyke, Maskwa Lake, southeastern Manitoba. Canadian Mineralogist, 30, 687–697.

Waldbaum, D.R. and Robie, R.A. (1970) An internal sample container for hydrofluoric acid solution calorimetry. Journal of Geology, 78, 736–741.

Wyart, J. (1941) Sur un cas de polymorphisme par passage progressif d'un arrangement cristallin a un autre plus symetrique observe sur la leucite. Comptes Rendus de l'Académie des Sciences Paris, 205, 1077–1079.

MANUSCRIPT RECEIVED JULY 10, 2001
MANUSCRIPT ACCEPTED DECEMBER 1, 2001
MANUSCRIPT HANDLED BY BARB DUTROW